



A Phase-Contrast MRI Study to Investigate the Interaction of the CSF Dynamic with the Intracranial CSF Distribution

Dallery, Florine ; Makki, Malek I ; Capel, Cyrille ; Gondry-Jouet, Cathrine ; Baledent, Olivier

Abstract: **PURPOSES:** Cine PC-MRI has shown that CSF oscillations increase with age, while the ratio between the CSF Oscillation in the aqueduct and the spinal canal is constant. Our aim was to test whether the CSF hydrodynamic can bring complementary information to study pediatric population with an increase of the CSF volume. **Material and Method:** Forty three patients, newborns and children (mean age: 31 ± 32 months; 5 days - 111 months) with an intracranial CSF volume increase (ventricular or/and subarachnoid spaces) underwent a morphological MRI along with cine PC-MRI to quantify CSF oscillations. We defined a ratio of the ventricular area to that of the intracranial subarachnoid spaces (CSFratio). We also determined an index called CSFdynamic, which equals the CSF aqueduct stroke volume (SVAq) divided by the cervical stroke volume (SVC2C3) at the level C2C3 in the spine. **RESULTS:** Twenty-three patients presented only ventricular dilatation: CSFdynamic = 20 ± 25 ; CSFratio: 120 ± 151 ; with no significant correlation, ($r_s = 0.152$, $p = 0.48$). Sixteen patients presented both ventricular and subarachnoid space dilations: CSFdynamic = 18 ± 17 ; CSFratio = 1.67 ± 0.81 ; with significant positive correlation ($r_s = 0.5911$, $p = 0.016$). **CONCLUSIONS:** In pediatric population, the absence of correlation between the dynamic of the CSF and its volume shows that the CSF oscillation does not result only of the size of the ventricles and/or the subarachnoid spaces. The CSF oscillations bring complementary information concerning the active aspect of the CSF.

Posted at the Zurich Open Repository and Archive, University of Zurich

ZORA URL: <https://doi.org/10.5167/uzh-138365>

Journal Article

Published Version



The following work is licensed under a Creative Commons: Attribution 3.0 Unported (CC BY 3.0) License.

Originally published at:

Dallery, Florine; Makki, Malek I; Capel, Cyrille; Gondry-Jouet, Cathrine; Baledent, Olivier (2017). A Phase-Contrast MRI Study to Investigate the Interaction of the CSF Dynamic with the Intracranial CSF Distribution. *JSM Neurosurgery and Spine*, 5(1):1079.

Review Article

A Phase-Contrast MRI Study to Investigate the Interaction of the CSF Dynamic with the Intracranial CSF Distribution

Florine Dallery^{1,2}, Malek Makki^{1,3*}, Cyrille Capel^{1,4}, Catherine Gondry-Jouet^{1,2}, and Olivier Balédent^{1,5}

¹Bio Flow Image, University of Picardie Jules Verne, France

²Department of Radiology, University Hospital of Picardie Jules Verne, France

³MRI Research, University Children Hospital of Zurich, Switzerland

⁴Department of Neurosurgery, University Hospital of Picardie Jules Verne, France

⁵Department of Image Processing, University Hospital of Picardie Jules Verne, France

*Corresponding author

Malek IMakki, MRI Research, University Children Hospital Zurich, Steinwiesstrasse 75, 8032 – Zurich, Switzerland, Tel: 41-444-266-3130; Fax: 41-44-266-7153; Email: malek.makki@kispi.uzh.ch

Submitted: 30 October 2016

Accepted: 04 February 2017

Published: 06 February 2017

Copyright

© 2017 Makki et al.

OPEN ACCESS

Keywords

- Hydrocephalus
- Subarachnoid space
- Ventricles
- PC-MRI
- Stroke volume

Abstract

Purposes: Cine PC-MRI has shown that CSF oscillations increase with age, while the ratio between the CSF oscillation in the aqueduct and the spinal canal is constant. Our aim was to test whether the CSF hydrodynamic can bring complementary information to study pediatric population with an increase of the CSF volume.

Material and Method: Forty three patients, newborns and children (mean age: 31 ± 32 months; 5 days - 111 months) with an intracranial CSF volume increase (ventricular or/and subarachnoid spaces) underwent a morphological MRI along with cine PC-MRI to quantify CSF oscillations. We defined a ratio of the ventricular area to that of the intracranial subarachnoid spaces (CSF_{ratio}). We also determined an index called $CSF_{dynamic}$, which equals the CSF aqueduct stroke volume (SV_{Aq}) divided by the cervical stroke volume (SV_{C2C3}) at the level C2C3 in the spine.

Results: Twenty-three patients presented only ventricular dilatation: $CSF_{dynamic} = 20 \pm 25$; $CSF_{ratio} = 120 \pm 151$; with no significant correlation, ($r_s = 0.152$, $p = 0.48$). Sixteen patients presented both ventricular and subarachnoid space dilations: $CSF_{dynamic} = 18 \pm 17$; $CSF_{ratio} = 1.67 \pm 0.81$; with significant positive correlation ($r_s = 0.5911$, $p = 0.016$).

Conclusion: In pediatric population, the absence of correlation between the dynamic of the CSF and its volume shows that the CSF oscillation does not result only of the size of the ventricles and/or the subarachnoid spaces. The CSF oscillations bring complementary information concerning the active aspect of the CSF.

ABBREVIATIONS

PC-MRI: Phase Contrast Magnetic Resonance Imaging; SV: Stroke Volume; SAS: Subarachnoid Space; CSF: Cerebrospinal Fluid

INTRODUCTION

The cerebrospinal fluid (CSF) is mainly located in the ventricular system in the brain and in the subarachnoid space (SAS) around it. In normal developing children, it is difficult to determine whether the expansion of both intra and peri brain fluid spaces is pathological or simply physiologically related to normal growing with age [1]. Some of these expansions have no influence

on growth and brain maturation, and may even eventually disappear [2], while others exert deleterious stress on the brain and require neurosurgery. In general, children who present high cranial perimeter, convulsive and cephalic crisis, meningitis, intra-ventricular or subarachnoidal hemorrhage, hypotonia or infection are suspected to have hydrocephaly caused by alteration of the CSF oscillation [3-5], and are referred for brain MRI. The oscillation of CSF is known to be altered in other pathologies including intracranial hypo- or hypertension [6], subarachnoidal haemorrhage [7], cerebral venous thrombosis [8], posterior fossa cystic malformations [9], and Alzheimer disease [10]. In addition, Chiari type I, Dandy Walker malformation, cerebral tumor, fewer resumption of the CSF following arachnoid's hemorrhage, or

meningitis can also obstruct the CSF flow [11]. The lack or absence of these clinical symptoms in neonates make the neurological diagnosis very difficult, particularly to differentiate between active hydrocephalus that requires surgical procedure (either endoscopic third ventriculostomy or ventriculoperitoneal shunt), and non-active hydrocephalus (i.e. brain atrophy, or normal CSF dynamic) that does not affect brain development. For growing children, age is considered a crucial parameter to evaluate the size of both the skull and the ventricles. However, the assessment of any enlargement is very challenging for neonates because the fontanel is not closed and the cerebral development is rapid with age [12]. Whether an increase of CSF volume is exclusively in the ventricles, or in the SAS, or both, is mainly based on qualitative visual observation. The lack of reliable, easy to use and accurate quantitative evaluation of these enlargements makes it difficult for neuro-radiologists to sharpen their diagnosis and report the severity of the disease. This might explain that, despite the involvement of the CSF oscillation in these pathologies, not that much attention has been given to study the dynamic of the CSF.

Flow-sensitive based MRI technique such as cine phase-contrast (PC-MRI) provides quantitative methods to study brain dynamic, in normal physiological conditions, and is increasingly used in clinical practice [13]. It has been performed to study blood dynamic [14,15] and cerebrospinal fluid (CSF) dynamic [16-18]. Such quantitative analysis of CSF flow and velocity brings complementary information to study brain hydrocephalus in children and neonates, and might have the necessary answer to separate between active and passive hydrocephalus and whether or not ventricular shunt is necessary [19].

Using this technique Capel et al., investigated the changes of CSF dynamic with age of typically developed children, and they reported an increase of the CSF stroke volume (volume displaced in 1 cardiac cycle $SV = mL/CC$) in the aqueduct and in the subarachnoid spaces with age to reach that of adult around one year of age [1]. They also show that cervical CSF stroke volume (at the level of C2C3) in healthy young children ($752 \cdot 10^{-3} mL/CC$) is almost 20 times larger than that of neonates ($38 \cdot 10^{-3} mL/CC$). At the same time, CSF stroke volume in the aqueduct increases by a factor of 10 (from 5 to $53 \cdot 10^{-3} mL/CC$). The CSF stroke volumes measured both in the aqueduct and in the cervical remain within the range of that of adults (respectively 37.5 ± 17.5 and $485 \pm 110 \mu L/CC$). The authors concluded also that the dynamic of cervical CSF was not significantly different before and after closure of the fontanels. In another study using PC-MRI, Bateman et al., showed a reversal of CSF global flows (net flow) in young hydrocephalus children (< 2 years) [19]. In older children, they demonstrated that the global CSF flows was in the expected direction, but seven times higher than that of control subjects [19]. More recent study reported a weak contribution of the ventricular system in response to vascular expansion [20] (~5%). Previous study has reported an alteration of the ventricular system in hydrocephaly [21], and it has been shown that a small CSF volume displacement in these compartments has a minor contribution to the instantaneous regulation of intracranial pressure (ICP). In infant brain, the cerebro-vascular expansion during the systolic phase is offset by both the compliance of the fontanels and the intracranial subarachnoid CSF flushing-out to spinal subarachnoid space. As

a result, a good communication between intracranial and spinal compartments of the CSF during the CC is crucial to avoid large increase of ICP amplitude. It has also been suggested that cervical CSF flushing out to the dural sac via the spinal subarachnoid spaces represents the main craniospinal compliance in front of the fontanels, and that any alteration of these spinal spaces might cause hydrocephalus development often seen in IVH newborns population [21].

From these previous studies, we conclude that 1) the correlation of CSF flow with age is not linear but rather follows a stepwise relationship; 2) the amplitude of the CSF oscillation with cardiac pulsations differs significantly in the SAS and the ventricles; 3) the CSF dynamic matures around 1 year of age in typically developed children, while brain morphology is still growing, making it difficult to assess any correlation at later age, and 4) the alteration of CSF flow is not homogenous is hydrocephaly. In addition it is not well established whether the underlying abnormal morphology observed in the ventricles and / or the SAS is of dynamics origin or whether a direct causality link exists between these 2 phenomena. This might explain the high failure neurosurgical interventions to treat hydrocephaly (either ETV or derivative valve): below 1% for neonates under 6 months of age, around 12.4% between 6 months and 1 year of age, 35.6% between 1 and 10 years of age, and 51.4% for children over 10 years of age [22,23]. Recently, an attempt to assess CSF flow in very complex structures such as the prepontine cistern to help identifying the appropriate candidate for endoscopic third ventriculostomy [24] has been applied by incorporating a saturation-pulse in 2D cine PC-MRI to suppress all artifacts related to blood aliasing from the basilar artery. Nevertheless, there is no PC-MRI technique dedicated to measuring the CSF dynamic in the SAS where the flow is turbulent and is sensitive to small velocity. Furthermore, these areas are surrounded by blood vessels that create aliasing artefact to low velocity encoding.

While hydrodynamic brain analysis of intra-ventricular CSF in adult population have found an interaction between high flow velocity in the aqueduct and normal pressure hydrocephalus [25-27], no such result has been found in children. Although we cannot extrapolate these findings to infants for brain morphology reasons (brain development and fontanel), we can still explore whether similar link might exist in children with hydrocephalus. It can be hypothesized that morphologic changes of the ventricles and/or the SAS during brain development constitute the primary cause to hydrocephalus and this leads to abnormal hydrodynamics. To further explore this idea, the current study aims to investigate whether an abnormal brain hydrodynamic and abnormal brain morphology are linked together. More specifically, first we would like to test the hypothesis that the dynamic of CSF differs between children with hydrocephalus and combined dilation of both the SAS and the ventricle, and children with hydrocephalus and ventricular dilation only. Second we want to investigate whether PC-MRI provided complementary information to that of morphologic images.

MATERIALS AND METHODS

Subjects

Forty-three patients (mean age = 31 ± 32 months, range = 5

days to 111 months) with intracranial increase of CSF volume were recruited. The increase in volume involves ventricular and/or SAS regardless of etiology. The inclusion criteria are children who had clinical neurology MRI in our University Hospital Center and are under 10 years of age with presence of a ventricular dilation without aqueduct stenosis on morphological sequences regardless of etiology (tumor, hemorrhage, infection, malformation, or unknown...). The patients were excluded if the clinical exam is not completed or invalid for clinical report.

These patients were divided in 3 subgroups:

The first group (Group1) includes 23 patients with ventricular dilation only; the second group (Group2) includes 16 children with both ventricular dilation and SAS dilation, and finally a group of 4 children with dilation of the SAS only (Group3). Further information about etiology was given along the number of patients in each category in Table (1). The French national ethical review board approved the study and all participant guardians gave their written consent.

Image acquisition

The study was performed on a 3T scanner (GE Healthcare, Milwaukee, WI, USA) using retrospectively and peripherally gated conventional cine PC-MRI to reconstruct 32 cardiac phases. The sequence was added to an existing MRI protocol and repeated at two levels: the aqueduct and the cervical spine C2C3 that includes. The clinical MRI includes sagittal T1W FLAIR, Axial T2W FLAIR, Axial T1W, Axial T2W, 3D T1 BRAVO, and high resolution T2W Fast-Spin-Echo 2D sequence covering the whole brain with the following imaging parameters: slice thickness = 5 mm, FOV=24x24 cm², TR=5500 to 6500 ms, TE= 80 to 120 ms, matrix: 480x480. The slices were positioned parallel to the ACPC line (Figure 1) so that they matched the anteroposterior axis of the lateral ventricle.

The 2D-PC imaging parameters are

Aqueduct: Slice thickness=5 mm, FOV=140x140 mm², phase FOV 75%, BW=62.5 kHz, flip angle=30°, minimum TE and TR, matrix 256x256, 2 views-per-segment, 2 repetitions, in an oblique oriented perpendicular to the direction of the CSF flow (Figure 1). The velocity encoding (*Venc*) of the conventional sequence was set to of 10 cm/s. The total acquisition time was about 1-2 min depending on heart rate.

Cervical: Slice thickness =5 mm, FOV=140x98 mm², BW=62.5 kHz, flip angle =30°, minimum TE and TR, matrix 256x256, 2 views-per-segment, 2 repetitions, and slice position at the level of the C2C3 and oblique oriented to be perpendicular to the direction of the CSF flow (Figure 1). The velocity encoding (*Venc*) of the conventional sequence was set to 10 cm/s. The total acquisition time was about 1 min.

1. To minimize SAR effect, three different coils were selected to perform this study on these children based either on their age or their wUnder 1 month: knee coil (Exciter/Receiver)
2. Under 10 Kg: Head coil (Exciter/Receiver)
3. Over 10 Kg: 8 channel head coil (Exciter/Receiver)

Processing morphologic t2w-fse images

The segmentation of the SAS and the ventricle was performed using dedicated free medical imaging software MIPAV (<http://mipav.cit.nih.gov/>) suited for automatic delineation of brain anatomy. To achieve our aims we used oblique axial planes to measure the area of the ventricles (*Ventricle_{area}*), the area of the skull (*Skull_{area}*) and the brain area (*Brain_{area}*) (Figure 2).

To assess the dilation of ventricle with regards to total brain area, we define a ventricular index *Ventricle_{ratio}* which

Table 1: Patient Group and Etiology - Distribution of patients per etiology (unknown, Tumor, Infection, Malformation and Hemorrhage) for each of the 3 groups.

Etiology	Tumor	Infection	Malformation	Hemorrhage	Unknown	Total
Group 1	1	2	11	4	5	23
Group 2	1	1	6	1	7	16
Group 3	0	0	1	1	2	4

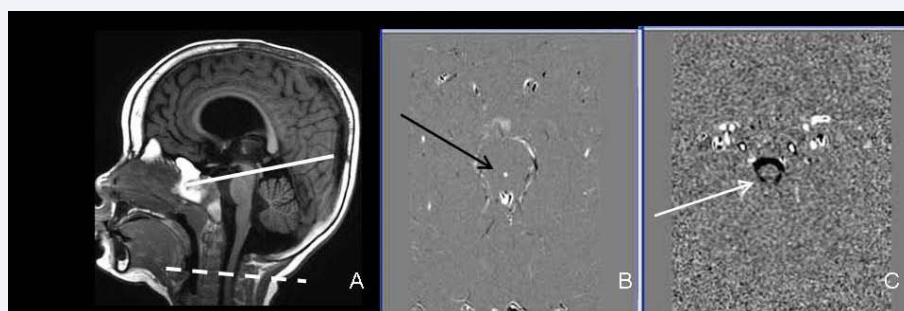


Figure 1 A) Sagittal scout image to display the slice positioning of PC-MRI perpendicular to the aqueduct (white line) and at the level of C2C3 (white dashed line). A phase-contrast image at one time point of the cardiac cycle (B) is obtained showing the aqueductal CSF flow direction (black arrows points to a white area demonstrating a cranio-caudal direction). C) A phase image at the cervical level showing a black rim (white arrow) demonstrating the caudo-cranial direction of the CSF flow.

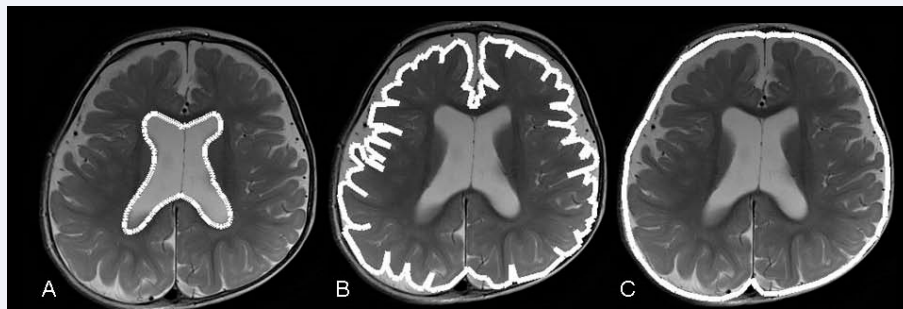


Figure 2 Morphological analysis with segmentations of measurements of the different areas achieved by the MIPAV software. (A): delineation and calculation of the of the ventricle areas; (B): delineation and calculation of the brain area; and (C): delineation and calculation of the skull area.

corresponds to the ratio of the ventricular area $Ventricle_{area}$ to the skull area $Skull_{area}$.

$$Ventricle_{ratio} = \frac{Ventricle_{area}}{Skull_{area}} \quad (1)$$

Similarly, to assess the dilation of the SAS area SAS_{area} with regards to total skull are $Skull_{area}$, we define a SAS index SAS_{ratio} which is the ratio of the 2 variables

$$SAS_{ratio} = \frac{SAS_{area}}{Skull_{area}} \quad (2)$$

Where $SAS_{area} = Skull_{area} - Brain_{area}$

From the 2 previous ratios, we assess the distribution of CSF in the ventricle with regard to SAS by introducing the ratio of the $Ventricle_{ratio}$ over the SAS_{ratio} . By performing this ratio the $Skull_{area}$ variable vanishes to obtain

$$CSF_{ratio} = \frac{Ventricle_{ratio}}{SAS_{ratio}} = \frac{Ventricle_{area}}{SAS_{area}} \quad (3)$$

Processing PC-MRI

Image processing was carried out using homemade software with dedicated CSF algorithm to segment and differentiate tissue with lower pulsatility than CSF, which is characterized by large amplitude oscillations [25]. The software uses "spectral segmentation" algorithm to extract a threshold value from the phase of the signal throughout the 32 cardiac phases. Then, an automatic and simultaneous delineation of CSF areas are performed separately in the aqueduct and the C2C3 level. Finally, the velocity and the flow values in each compartment through each cardiac phase are measured (Figure 2). The oscillation of CSF with cardiac cycle is composed in 2 parts: the caudo-cranial flow (minimum negative value) and the cranio-caudal flow (maximum positive value). The stroke volume (SV) was defined as the average of cranio-caudal and caudo-cranial volumes displaced through the region of interest during one CC (expressed in $\mu\text{l}/\text{CC}$). In fact, this corresponds to the area under the curve of the flow measures vs cardiac phases. To investigate the dynamic of the CSF, or the CSF flashing in and out of both the ventricle and the SAS through one cardiac cycle, we calculate the ratio of SV in the aqueduct SV_{Aq} to that of the cervical SV_{C2C3} :

$$CSF_{dynamic} = \frac{SV_{Aq}}{SV_{C2C3}} \quad (4)$$

Statistical analysis

We performed a simple Spearman's rho test for correlation of both $CSF_{dynamic}$ and CSF_{ratio} with age, and we reported the regression coefficient (Rs) and significance p . The age effect on the dilation of the SAS area was assessed by a ROC curve defined by the Kolmogorov-Smirnov test. When age correlates significantly with age, we performed partial correlation controlling for age to assess whether there is any correlation between two variables.

Group comparisons Group1 (ventricular dilation) versus Group2 (ventricular +SAS dilations) was carried out using MANCOVA (multiple analyses with covariance) for each parameter: CSF_{Aq} , CSF_{ratio} , SV_{Aq} , CV_{C2C3} , and age a MRI was introduced as covariate. The threshold significance was set to 0.05. The small sample size of Group3 (N=4) does not allow for any statistical analysis thus it was excluded from the comparisons.

RESULTS AND DISCUSSION

Age correlation

Spearman's rho test demonstrated that in both groups Group1 (ventricular dilation only) and Group2 (ventricular and SAS dilation) the area of the skull ($Skull_{area}$) and the area of the brain ($Brain_{area}$) positively correlate with age. It also showed that both stroke volumes at the aqueduct (SV_{Aq}) and at cervical (SV_{C2C3}) correlate positively with age (Table 2). Ventricle area ($Ventricle_{area}$) was positively correlated with age in Group2 only and not in Group1.

Partial correlation with age as covariate

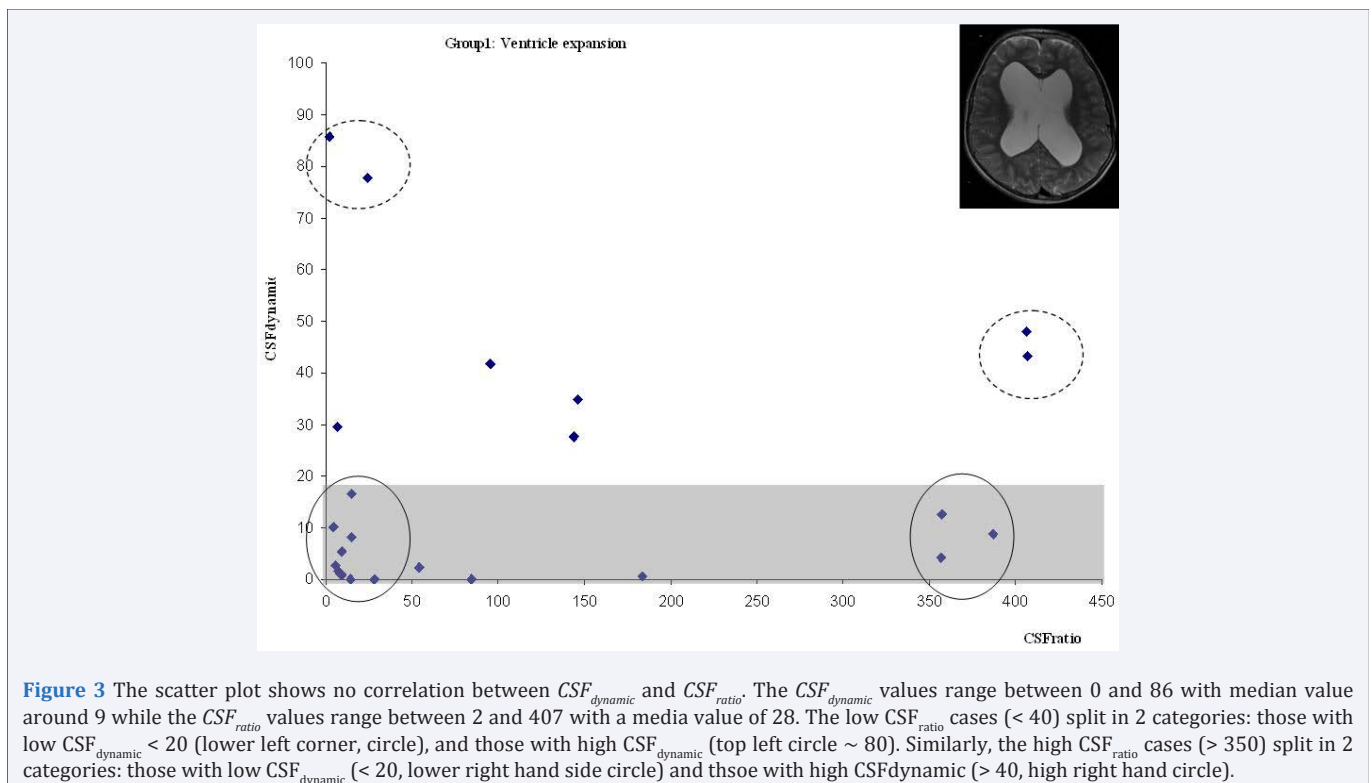
We performed partial correlation controlling for age at MRI separately for each group and included $Ventricle_{ratio}$, SAS_{ratio} , CSF_{ratio} , SV_{Aq} , SV_{C2C3} and $CSF_{dynamic}$ as variables (Table 3).

In both groups, we found a significant negative correlation between CSF_{ratio} and SAS_{ratio} and a significant positive correlation between $CSF_{dynamic}$ and SV_{Aq} . The CSF_{ratio} has significant positive correlation with SV_{Aq} in Group1 and with $Ventricle_{ratio}$ in Group2.

In Group1, the scatter plots (Figure 3) shows that there is no

Table 2: Spearman Rho correlation of the defined CSF indices with age at MRI - Spearman's rho correlation of the defined variables with age in both groups. Group1 refers to 23 patients with ventricular dilation, and Group2 refers to 16 patients with both ventricular and subarachnoidal space dilations. Significance was set to $p = 0.05$, and R is the correlation coefficient. The abbreviation "NS" stands for non significant.

Correlation with Age Spearman's rho	Ventricle dilation		Ventricle and SAS dilations	
	R	P	R	p
Skull _{area}	0.707	< 0.001	0.743	0.001
Brain _{area}	0.733	< 0.001	0.768	0.001
SV _{Aq}	0.572	0.004	0.764	0.001
SV _{C2C3}	0.785	<0.001	0.587	0.017
Ventricle _{area}	NS	NS	0.761	0.001



correlation between $CSF_{dynamic}$ and CSF_{ratio} . In the opposite, Group2 demonstrates a positive correlation between the 2 variables (Figure 4), which can be explained either by an increase of CSF oscillations through the aqueduct or a decrease of the dynamic in the cervical (C2C3).

The second observation is that the range of the $CSF_{dynamic}$ value is almost the same for both groups. In Group1 (ventricular dilation) the values range between 0 and 86 (median=9), and in Group2 (ventricle + SAS dilations) the values range between 3 and 71 (median=12). Thus we can report that, for children with hydrocephaly, the ratio of SV_{Aq} to SV_{C2C3} (aqueduct to cervical stroke volume) remains within the same range (min 0, max 86, median=10) no matter whether the dilation is located in the ventricle only or in both the ventricle and the SAS.

In Group1 (Figure 3), the CSF_{ratio} values range between 2 and 407 (median=28), and in Group2 (Figure 4), the range is between 0 and 3 (median=2), so there is a factor of 1 to 100 between the two groups. In typically developed children, the $CSF_{dynamic}$ has been found around 16 ± 9 . In Group1 we observed a category of

patients who have $CSF_{dynamic}$ within these normal value (~20), and another category of patients with very high value (~80). Each category of children splits in 2 subgroups: one with very low CSF_{ratio} (<50) and those with very high CSF_{ratio} (>300).

Group differences

The age of Group1 (mean = 38.24 ± 7.97 months) and the age of Group2 (mean = 11.78 ± 2.95 months) were significantly different ($p = 0.002$). For this reason, between groups MANCOVA was performed with age at MRI as covariate. The test showed that Group1 has a significantly higher $Ventricle_{area}$ ($p=0.033$), a significant higher $Ventricle_{ratio}$ ($p=0.004$), a significantly lower SAS_{area} ($p<0.001$) and a significantly lower SAS_{ratio} ($p<0.001$) compared to Group2. None of the other differences reached significance, but noteworthy to mention that there was a trend toward higher CSF_{ratio} ($p=0.05$) in Group1 compared to Group2 (Table 4).

DISCUSSION

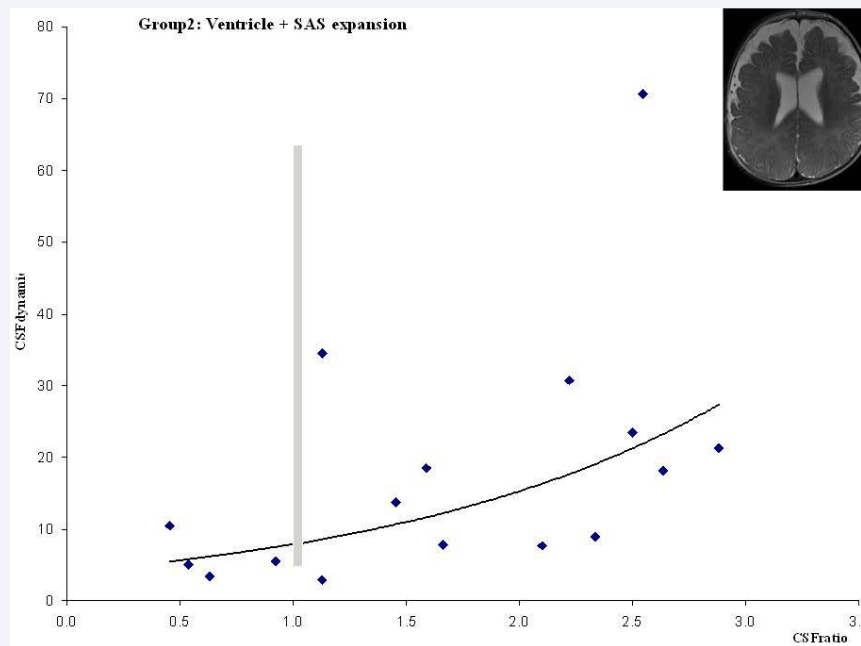


Figure 4 The correlation curve shows an exponential growth of $CSF_{dynamic}$ with CSF_{ratio} . The $CSF_{dynamic}$ values range between 3 and 71 with median value around 12 while the CSF_{ratio} values range between 0 and 3 with a media value of 2. The grey line indicates the $CSF_{ratio} = 1.0$ which implies identical $Ventricle_{area}$ and SAS_{area} .

Table 3: Bivariate Partial correlation Controlling for age at MRI of the defined CSF indices - Bivariate correlation controlling for age at MRI in both groups: Group1 includes 23 patients with ventricular dilation only while Group2 includes 16 patients with both ventricular and subarachnoidal space dilations. Significance was set to $p = 0.05$, and R is the correlation coefficient. The sign "--" stands for non significant.

Partial correlation Controlling for age	Ventricle dilation Group1		Ventricle and SAS dilations Group2	
	R	P	R	P
CSF_{ratio} & SAS_{ratio}	-0.602	0.002	-0.701	0.004
CSF_{ratio} & $Ventricle_{ratio}$	NS	NS	0.645	0.009
CSF_{ratio} & SV_{Aq}	0.445	0.038	NS	NS
$CSF_{dynamic}$ & SV_{Aq}	0.531	0.011	0.775	0.001
$CSF_{dynamic}$ & SV_{C2C3}	NS	NS	NS	NS

Table 4: Between group differences of the defined CSF indices - Between groups difference was performed with general linear model MANCOVA using age at MRI as covariate. Significance was set to $p = 0.05$. The abbreviation "NS" stands for non-significant.

Group differences Age as covariate	Ventricle dilation Mean \pm SE	Ventricle and SAS dilations Mean \pm SE	p
$Ventricle_{area}$ [mm^2]	3575 \pm 472	2054 \pm 264	0.033
SAS_{area} [mm^2]	218 \pm 45	1360 \pm 159	< 0.001
$Ventricle_{ratio}$	0.2503 \pm 0.029	0.1231 \pm 0.0147	0.004
SAS_{ratio}	0.015 \pm 0.003	0.094 \pm 0.0098	<0.001
CSF_{ratio}	104.7 \pm 31.5	23.77 \pm 0.20	0.052
$CSF_{dynamic}$	20.2 \pm 5.2	17.63 \pm 4.3	NS

This study of the CSF of children with hydrocephaly includes 2 groups of patients: Group1 involves ventricle enlargement only and Group2 with enlargement of both the ventricle and the SAS. We have shown that in both groups, there is a positive correlation of skull area, brain area, aqueduct stroke volume, and cervical stroke volume with age. These increases with age exist in typically developed children as well which make it difficult

for clinicians to assess whether or not the increase is within normality based on qualitative observation only. This confirms the need for complementary indices because longitudinal study on brain size of hydrocephalic patients does not exist. We also observed that the positive correlation of ventricle area with age is lost among patient with ventricle enlargement only mainly due to substantial abnormal increase of the CSF volume exclusively

in these structures. We also found that, in patients with ventricle enlargement only (Group1), the distribution of CSF in the ventricle relative to the SAS (expressed by CSF_{ratio}) increases significantly either with an increase of the stroke volume in the aqueduct (SV_{Aq}) or with a decrease of the SAS ratio, but it is not significantly affected by the relative change in the ventricle area. In these patients, the dynamic of the CSF (flow thru the aqueduct / flow thru the SAS) increases with the stroke volume in the aqueduct but not in the cervical. Overall, there was no association between the dynamic of the CSF (relative flow thru the aqueduct to the SAS expressed by $CSF_{dynamic}$) and the distribution of the CSF in the ventricle relative to the SAS (CSF_{ratio}). In this group, we observe that the size of CSF compartments does not directly correlate with the CSF dynamic. All patients in this group presented an abnormal pathological CSF volume dilation and the ratio of ventricle dilation ranged between $2 \times SAS_{area}$ to $\sim 400 \times SAS_{area}$. There is a category of children who had normal CSF dynamic (lower than 20) regardless of the CSF volume distribution between the ventricles and the SAS ($CSF_{ratio} < \text{median value of } 28$, or even $CSF_{ratio} > 300$). Interestingly, among the other category of patients with pathological brain hydrodynamic ($CSF_{dynamic} > 20$), we also observed 2 subgroups of patients: the 1st subgroup with small CSF repartition between the SAS and the ventricles ($CSF_{ratio} < 28$) while the 2nd subgroup presented very high ratio (> 100). Based on the pioneer works of Marmarou et al., the CSF pressure-volume relationship in the cranium has an exponential trajectory [28]. The intracranial pressure (ICP) in response to uncompressed rapid changes in intracranial blood, brain, and CSF volume (ΔV) has 3 stages as a function of the compliance ($C = \Delta V / \Delta P$). In stage I there is a large compensatory reserve at low IPC where any change in volume produces negligible or little change of the pressure, eg maximum compliance. This phase corresponds to patients who have normal CSF drainage ($CSF_{dynamic} < 20$) with very active compensatory system and maximum compliance at low CSF_{ratio} . In patients with high CSF_{ratio} and normal $CSF_{dynamic}$ there is probably a high capacity of the cerebral auto regulation and more arterioles dilation in respond to any additional increase of the ICP. These characteristics match with the stage III of the pressure-volume curve where the brain reaches the limit of the cerebral auto regulation capacity and cerebral arterioles dilate in respond to any additional increase of the ICP. At stage II or the pressure-volume curve, e.g. the steep part, the compensatory reserve is low so that any small increase in the volume generates a fast increase in the ICP, eg low compliance. This part of the curve corresponds to patients with high $CSF_{dynamic}$ (> 20) with low CSF_{ratio} . It has been shown that CSF absorption takes place about 85% within the cerebral compartment [19]. The low absorption value in the spinal compartment suggests that loss of communication between cerebral and spinal compartments should have negligible effect on the steady-state level of the ICP [28].

The last group of patients with abnormally high brain dynamic and high CSF_{ratio} , this corresponds to a break thru of the limit of the cerebral autoregulation capacity and cerebral arterioles dilate in respond to any additional increase of the ICP. For these patients cerebrovascular deterioration happens more frequently when ventricles close due to brain edema or contusion occupies more space in the cranium [29]. In the case of closed

head injury it has been shown that the degree of correlation between the amplitude of the fundamental component and the mean ICP (RAP) is associated with the width of the ventricle and negatively with the total volume of contusions [30].

In patients with a combined expansion of the ventricle and the SAS (Group2), an exponential relationship has been found between the CSF dynamic and the CSF volume distribution. The CSF distribution increases significantly with a decrease of the distribution in the SAS (similar to Group1), but increases with the CSF distribution in the ventricle (unlike Group1). In these patients the stroke volume thru the aqueduct is not linked to the distribution of the CSF (unlike Group1), but it is associated to the dynamic of the CSF. We did not find any association between the dynamic of the CSF ($CSF_{dynamic}$) and the relative CSF distribution in the ventricle and the SAS areas (CSF_{ratio}) in these patients (similar to Group1).

From these findings, we conclude that in hydrocephaly with ventricle enlargement only, the SAS plays a minor role in the dynamic of the CSF, despite the association between the CSF volume and the area of the skull. This is in line with previous finding by Stephensen H et al., who observed that there is no pressure gradient between the ventricles and the cranial SAS in non-communicating hydrocephalus [31]. Other studies in patients with brain atrophy have shown that there was no correlation between the amplitude of ICP and the arterial pulse pressure, which suggests that there is no vasogenic variation, while a strong positive correlation has been reported in patients with normal pressure hydrocephaly [32]. The positive correlation of CSF_{ratio} with the stroke volume at the aqueduct (SV_{Aq}) in Group1 means that in these patients, where the distribution of CSF is high in the ventricles, and the brain dynamic compensatory system is active, the compliance phenomenon is low which leads to very high differential ΔP .

The positive correlation between the aqueduct stroke volume and the CSF volume in Group1, but not in Group2, points to the importance of the CSF circulation thru this canal for patients with ventricular enlargement but to fewer expanses for patients who present both dilations. These results are in concordance with other findings which demonstrated that an increase in pulse amplitude is not a factor promoting ventricular dilation [30]. Furthermore, Czosnyka et al., suggested that that greater pulse amplitude is associated with weaker autoregulation [33].

The important role of the aqueduct stroke volume (SV_{Aq}) compared to cervical stroke volume (SV_{C2C3}) is further highlighted by the correlation with the CSF dynamic ($CSF_{dynamic}$) in both groups, while there is no correlation with SV_{C2C3} neither in Group 1 nor in Group2. In these patients, our results showed that CSF_{ratio} correlates positively with $Ventricle_{ratio}$ and negatively with SAS_{ratio} . This means that, in Group2, the expansion of the SAS plays a crucial role in the enlargement of the skull, and to less extend in Group1. Similar conclusion was highlighted in idiopathic normal pressure hydrocephaly, where lower pulse amplitude was measured in the ventricles compared to lumbar space, and it has been concluded that there is no evidence of association between pulse amplitude and a dilation of the ventricle [30].

The analysis of the curve $CSF_{dynamic}$ versus CSF_{ratio} shows

that, in patients with a ventricle dilation combined to a SAS expansion (Group2), there is a direct positive relationship between CSF flow and the size of CSF compartments. Any increase of the CSF ventricular distribution in the ventricle compartment ($Ventricle_{area}$) relative to the subarachnoid space (SAS_{area}) correlates with an increase of CSF oscillations through the aqueduct. This was observed regardless of the CSF_{ratio} value (higher or lower than one) and means that in these patients, the compensatory compliance system is distributed between the 2 compartments. These results confirm the findings from earlier studies suggesting that the total CSF compliance can be subdivided into 2 compartments: cerebral which includes vascular elements (~2/3 of the total compliance) and spinal components [34]. This means that the cerebral compartment is more susceptible to increase of pressure due to the fluctuations in volume [28,35]. Although further studies are needed with a larger population and a longitudinal follow-up to evaluate these trends between new morphological and dynamic parameters, one can highlight the complementary information that PC-MRI adds to morphological imaging.

This study has few limitations that are mainly related to spatial resolution that needs improvement to provide more efficiency in the segmentation and measurement in relatively small compartments. The trade off is higher temporal resolution and decreased SNR that by itself is already a limitation that needs also to be addressed. The eddy-current effect and concomitant magnetic field are also a limitation that needs to be sorted out at the acquisition. To overcome this we assume that the static tissue has zero phase shifts and there is no difference between 2 consecutive sequences. The sample size of each group is a limitation and a larger group might increase the sensitivity of the findings and the trend towards significance.

CONCLUSION

We have shown that using a fast single-slice based PC-MRI acquisition we can measure the CSF oscillations during cardiac cycle in the aqueduct and the cervical spaces in newborn and children. We suggest a segmentation technique and a quantification method simple to use and accessible to pediatric neurology and radiology. In our study, all patients have an abnormal CSF volume dilatation with either normal or pathologic CSF dynamic. Our findings show that the size of the CSF compartments is not directly correlated to the CSF dynamic. A study with larger population is necessary to confirm these preliminary results and to demonstrate the usefulness of quantitative PC-MRI that adds complementary information's to morphological imaging. This study provides new insights into brain CSF dynamic and such data is vital to help clinicians to better diagnose and interpret patients who present an active hydrocephalus requiring shunt.

ACKNOWLEDGEMENTS

We are very grateful to the Chiari & Syringomyelia foundation for funding the Cerebrospinal Fluid Dynamics Symposium 2015 (<http://csfdynamics.org/>) that brought scientists from around the world that helped us in the final discussion of the findings.

REFERENCES

1. Capel C, Makki M, Gondry-Jouet C, Bouzerar R, Courtois V, Krejpcowicz B, et al. Insights into cerebrospinal fluid and cerebral blood flows in infants and young children. *J Child Neurol*. 2014; 29: 1608-1615.
2. Suara RO, Trouth AJ, Collins M. Benign subarachnoid space enlargement of infancy. *J Natl Med Assoc*. 2001; 93: 70-73.
3. Bradley WG, Scalzo D, Queralt J, Nitz WN, Atkinson DJ, Wong P. Normal-pressure hydrocephalus: evaluation with cerebrospinal fluid flow measurements at MR imaging. *Radiology*. 1996; 198: 523-529.
4. Mase M, Yamada K, Banno T, Miyachi T, Ohara S, Matsumoto T. Quantitative analysis of CSF flow dynamics using MRI in normal pressure hydrocephalus. *Acta Neurochir Suppl*. 1998; 71: 350-353.
5. Miyai T, Mase M, Banno T, Kasuga T, Yamada K, Fujita H, et al. Frequency analyses of CSF flow on cine MRI in normal pressure hydrocephalus. *Eur Radiol*. 2003; 13: 1019-1024.
6. Tain RW, Bagci AM, Lam BL, Sklar EM, Ertl Wagner B, Alperin N. Determination of cranio-spinal canal compliance distribution by MRI: Methodology and early application in idiopathic intracranial hypertension. *J Magn Reson Imaging*. 2011; 34: 1397-1404.
7. Saliou G, Paradot G, Gondry C, Bouzerar R, Lehmann P, Meyers ME, et al. A Phase-contrast MRI study of acute and chronic hydrodynamic alterations after Hydrocephalus Induced by Subarachnoid Hemorrhage. *J Neuroimaging*. 2012; 22: 343-350.
8. Elsankari S, Czosnyka M, Lehmann P, Meyer ME, Deramond H, Balédent O. Cerebral Blood and CSF Flow Patterns in Patients Diagnosed for Cerebral Venous Thrombosis - An Observational Study. *J Clin Imaging Sci*. 2012; 2: 41.
9. Yildiz H, Yazici Z, Hakyemez B, Erdogan C, Parlak M. Evaluation of CSF flow patterns of posterior fossa cystic malformations using CSF flow MR imaging. *Neuroradiology*. 2006; 48: 595-605.
10. Sankari El S, Gondry-Jouet C, Fichten A, Godefroy O, Serot JM, Deramond H, et al. Cerebrospinal fluid and blood flow in mild cognitive impairment and Alzheimer's disease: a differential diagnosis from idiopathic normal pressure hydrocephalus. *Fluids Barriers CNS*. 2011; 8: 12.
11. Leliefeld PH, Gooskens RH, Vincken KL, Ramos LM, van der Grond J, Tulleken CA, et al. Magnetic resonance imaging for quantitative flow measurement in infants with hydrocephalus: a prospective study. *J Neurosurg Pediatr*. 2008; 2: 163-170.
12. Eskandari R, Melissa Packer, Burdett EC, Mcallister JP. Effects of Early and Late Reservoir Treatment in Experimental Neonatal Hydrocephalus. *Int Soc Pediatr Neurosurg*. 2012; 28: 1849-1861.
13. Feinberg DA, Mark AS. Human brain motion and cerebrospinal fluid circulation demonstrated with MR velocity imaging. *Radiology*. 1987; 163: 793-799.
14. Enzmann DR, Ross MR, Marks MP, Pelc NJ. Blood flow in major cerebral arteries measured by phase-contrast cine MR. *AJNR Am J Neuroradiol*. 1994; 15: 123-129.
15. Binkert CA, Debatin JF, Schneider E, Hodler J, Ruehm SG, Schmidt M, et al. Can MR Measurement of Renal Artery Flow and Renal Volume Predict the Outcome of Percutaneous Transluminal Renal Angioplasty? *Cardiovasc Intervent Radiol*. 2001; 24: 233-239.
16. Enzmann DR, Pelc NJ. Normal flow patterns of intracranial and spinal cerebrospinal fluid defined with phase-contrast cine MR imaging. *Radiology*. 1991; 178: 467-474.
17. Pelc NJ. Flow quantification and analysis methods. *Magn Reson Imaging Clin N Am*. 1995; 3: 413-424.
18. Baledent O, Gondry-Jouet C, Stoquart-Elsankari S, Bouzerar R, Le Gars D, Meyer ME. Value of phase contrast magnetic resonance imaging

- for investigation of cerebral hydrodynamics. *J Neuroradiol.* 2006; 33: 292-303.
19. Bateman GA, Brown KM. The measurement of CSF flow through the aqueduct in normal and hydrocephalic children: from where does it come, to where does it go? *Childs Nerv Syst.* 2012; 28: 55-63.
 20. Capel C, Kasprovicz M, Czosnyka M, Baledent O, Smielewski P, Pickard JD, et al. Cerebrovascular time constant in patients suffering from hydrocephalus. *Neurol Res.* 2014; 36: 255-261.
 21. Baledent O, Gondry-Jouet, Meyer ME. Relationship between Cerebrospinal Fluid and Blood Dynamics in Healthy Volunteers and Patients with Communicating Hydrocephalus. *Invest Radiol.* 2004; 39: 45-55.
 22. Drake JM. Canadian Pediatric Neurosurgery Study Group. Endoscopic third ventriculostomy in pediatric patients: the Canadian experience. *Neurosurgery.* 2007; 60: 881-886.
 23. Lam S, Harris D, Rocque BG, Ham SA. Pediatric endoscopic third ventriculostomy: a population-based study. *J Neurosurg Pediatr.* 2014; 14: 455-464.
 24. Ruegger CM, Makki MI, Capel C, Gondry-Jouet C, Baledent O. An innovative approach to investigate the dynamics of the cerebrospinal fluid in the prepontine cistern: A feasibility study using spatial saturation-prepared cine PC-MRI. *Eur J Radiol Open.* 2014; 1: 14-21.
 25. Balédent O, Henry-Feugeas MC, Idy-Peretti I. Cerebrospinal fluid dynamics and relation with blood flow: a magnetic resonance study with semiautomated cerebrospinal fluid segmentation. *Invest Radiol.* 2001; 36: 368-377.
 26. Bradley WG, Scalzo D, Queralt J, Nitz WN, Atkinson DJ, Wong P. Normal-pressure hydrocephalus: evaluation with cerebrospinal fluid flow measurements at MR imaging. *Radiology.* 1996; 198: 523-529.
 27. Luetmer PH, Huston J, Friedman JA, Dixon GR, Petersen RC, Jack CR, et al. Measurement of cerebrospinal fluid flow at the cerebral aqueduct by use of phase-contrast magnetic resonance imaging: technique validation and utility in diagnosing idiopathic normal pressure hydrocephalus. *Neurosurgery.* 2002; 50: 534-544.
 28. Marmarou A, Shulman K, LaMorgese J. Compartmental analysis of compliance and outflow resistance of the cerebrospinal fluid system. *J Neurosurg.* 1975; 43: 523-534.
 29. Hiler M, Czosnyka M, Hutchinson P, Balestreri M, Smielewski P, Matta B, et al. Predictive value of initial computerized tomography scan, intracranial pressure, and state of autoregulation in patients with traumatic brain injury. *J Neurosurg.* 2006; 104: 731-737.
 30. Czosnyka M, Smielewski P, Timofeev I, Lavinio A, Guazzo E, Hutchinson P, et al. Intracranial pressure: more than a number. *Neurosurg Focus.* 2007; 22: 10.
 31. Stephensen H, Tisell M, Wikkelsö C. There is no transmantle pressure gradient in communicating or noncommunicating hydrocephalus. *Neurosurgery.* 2002; 50: 763-773.
 32. Eide PK, Brean A. Intracranial pulse pressure amplitude levels determined during preoperative assessment of subjects with possible idiopathic normal pressure hydrocephalus. *Acta Neurochir (Wien).* 2006; 148: 1151-1156.
 33. Czosnyka M, Czosnyka Z, Keong N, Lavinio A, Smielewski P, Momjian S, et al. Pulse pressure waveform in hydrocephalus: what it is and what it isn't. *Neurosurg Focus.* 2007; 22: 2.
 34. Katzman R, Hussey F. A simple constant-infusion manometric test for measurement of CSF absorption. I. Rationale and method. *Neurology.* 1970; 20: 534-544.
 35. Lim ST, Potts DG, Deonaraine V, Deck MD. Ventricular compliance in dogs with and without aqueductal obstruction. *J Neurosurg.* 1973; 39: 463-473.

Cite this article

Dallery F, Makki M, Capel C, Gondry-Jouet C, Balédent O (2017) A Phase-Contrast MRI Study to Investigate the Interaction of the CSF Dynamic with the Intracranial CSF Distribution. *JSM Neurosurg Spine* 5(1): 1079.